

WHOLE EARTH TELESCOPE OBSERVATIONS AND SEISMOLOGICAL ANALYSIS OF THE COOL ZZ CETI STAR GD 154

B. Pfeiffer^{1,3}, G. Vauclair¹, N. Dolez¹, M. Chevreton², J.-R. Fremy²,
M.A. Barstow^{3,11}, J.A. Belmonte⁴, S.O. Kepler⁵, A. Kanaan⁵, O.
Giovannini⁵, G. Fontaine^{6,12}, P. Bergeron^{6,12}, F. Wesemael^{6,12},
A.D. Grauer⁷, R.E. Nather⁸, D.E. Winget⁸, J. Provencal^{8,13}, J.C.
Clemens^{8,14}, P. Bradley^{8,15}, J.S. Dixon⁸, S.J. Kleinman⁸, T.K.
Watson⁸, C.F. Claver⁸, T. Mazeh⁹, E.M. Leibowitz⁹, P. Moskalik¹⁰

¹ *Observatoire Midi-Pyrénées, Laboratoire d'Astrophysique de Toulouse,
14 Ave. E. Belin, 31400 Toulouse, France*

² *Observatoire de Paris-Meudon, 92195 Meudon, France*

³ *Department of Physics and Astronomy, University of Leicester, LE1
7RH, U.K.*

⁴ *Instituto Astrofísico de Canarias, Via Lactea S/N, E-38200,
La Laguna, Tenerife, Spain*

⁵ *Instituto de Física, Universidade Federal do Rio Grande do Sul, 91501-
970 Porto Alegre, RS, Brazil*

⁶ *Département de Physique, Université de Montréal, CP6128, Succursale
A, Montréal, Québec, H3C 3J7, Canada*

⁷ *Department of Physics and Astronomy, University of Arkansas,
Little Rock, AR 72204, U.S.A.*

⁸ *Department of Astronomy, University of Texas, Austin, TX 78712,
U.S.A.*

⁹ *Department of Physics and Astronomy, Tel Aviv University,
Tel Aviv 69978, Israel*

¹⁰ *Copernicus Astronomical Center, ul. Bartycka 18, 00-716
Warsaw, Poland*

¹¹ *Guest observer, Isaac Newton Telescope, Roque de Los Muchachos,
La Palma, Spain*

¹² *Guest observer, Canada-France-Hawaii Telescope, Mauna Kea,
Hawaii, U.S.A.*

¹³ *Present address: University of Delaware, Physics and Astronomy
Department, Sharp Lab., Newark, DE 19716, U.S.A.*

¹⁴ *Present address: Department of Physics, Iowa State University, Ames, IA 50011, U.S.A.*

¹⁵ *Present address: X-2, MS B-220, Los Alamos National Laboratory, Los Alamos, NM 87545, U.S.A.*

Received September 1, 1995.

Abstract. Fast photometric observations of a cool DAV star, GD 154, obtained with the Whole Earth Telescope are presented. GD 154 is one of the coolest pulsating DA white dwarfs and its study is relevant for understanding of the red edge of the ZZ Ceti instability strip. Its power spectrum is dominated by three independent modes ($P_1 = 1186.5$ s, $P_2 = 1088.6$ s and $P_3 = 402.6$ s). It also exhibits harmonics and linear combinations of these three modes. However, none of the half-integer harmonics, reported in previous observations, were present during the WET campaign. Assuming that the observed modes are trapped in the thin outer hydrogen layer, an identification of the pulsation modes is proposed. The rotation period (2.3 days) and the mass of the outer hydrogen layer ($2 \times 10^{-10} M_\star$) are derived.

Key words: stars: interiors – stars: oscillations – stars: pulsations – stars: structure – stars: individual: GD 154

1. Introduction

GD 154 (BG CVn) is a member of the class of pulsating white dwarfs known as the ZZ Ceti (or DAV) stars, which display intrinsic luminosity variations of a few percent and periods ranging between 100 and 1200 s. Only 24 ZZ Ceti stars are presently known. The DAV instability strip is delineated by a narrow range in effective temperature along the white dwarf cooling sequence: $12\,460\text{ K} \geq T_{\text{eff}} \geq 11\,160\text{ K}$ according to the $ML2/\alpha = 0.6$ models of Bergeron et al. (1995). The properties of the ZZ Ceti stars have been summarized by Winget and Fontaine (1982) and Winget (1988).

The variability of GD 154 was discovered by Robinson et al. (1978). They found that the light curve during nine consecutive nights was dominated by a single mode of moderate amplitude at frequency f_1 and a period $P_1 = 1186$ s. Such a long period was suggested to belong to a high overtone g-mode ($10 \leq k \leq 30$). The power spectrum exhibited harmonics of this dominant mode ($2f_1, 3f_1, 4f_1$ and $5f_1$). It also showed a series of peaks at frequencies close to half-integer subharmonics of the dominant mode ($1.52f_1, 2.53f_1$ and

$3.53f_1$). In addition, during the last night of their ten days campaign, the light curve of GD 154 was dominated by the $1.52f_1$ mode. This is reminiscent of some non linear dynamical systems behavior.

The occurrence of half integer subharmonics of the dominant frequency is similar to what is observed in systems evolving toward a chaotic dynamical regime via a cascade of period doubling bifurcations. Such a behavior has already been suspected from the analysis of the power spectrum of pulsating white dwarf in two cases: for the DBV PG1351+489 (Winget et al. 1987, Goupil et al. 1988) and the DAV G191-16 (Vauclair et al. 1989). The drastic change of the dominant frequency from f_1 to $1.52f_1$ observed by Robinson et al. (1978) also points to the potential efficiency in GD 154 of mechanisms responsible for exchanging energy between these two modes, possibly through non-linear effects. An alternative explanation in terms of beating between regularly spaced frequencies of the $\ell = 4$ mode has been suggested by O'Donoghue (1986). The peculiarities of its power spectrum were a strong motivation to propose that a Whole Earth Telescope campaign should be devoted to GD 154.

Furthermore, GD 154 presents some other interesting peculiarities as a member of the DAV class. It is one of the coolest ZZ Ceti stars. Based on the Balmer lines profile fitting procedure, Daou et al. (1990) determined an effective temperature of 11 320 K. The fitting of the UV flux (IUE) resulted in a temperature hotter by ~ 400 K (Kepler and Nelan 1993). More recently, Bergeron et al. (1995) demonstrated how an internally consistent determination of both the effective temperature and the surface gravity requires the simultaneous fitting of optical and UV spectra. They showed how a unique version of the mixing length theory successfully achieved this requirement with $ML2/\alpha=0.6$. According to their analysis, GD 154, with an effective temperature of 11 180 K, belongs to a group of three ZZ Ceti stars, which defines the red edge of the instability strip (with R 808 and G 38-29 at $T_{\text{eff}} = 11\,160$ K and 11 180 K, respectively).

The derived mass of GD 154 is $0.70 M_{\odot}$, a mass significantly higher than the average mass of DA white dwarfs (Bergeron et al. 1995). It is also most massive of the three ZZ Ceti stars defining the red edge.

The period of its dominant mode is the longest period up to now observed in DAV (1186 s). It is significantly longer than the periods of the dominant modes in G 38-29 (1024 s) and R 808 (833 s). Note that for the three stars defining the red edge, there is no apparent correlation between their mass and their location in the H-R diagram:

the red edge does not seem to depend on the total mass of stars (Bergeron et al. 1995). If it is assumed that the observed modes are trapped modes in the hydrogen outer layers, the longer period in GD 154 compared to other stars of the same effective temperature may have three different origins (Brassard et al. 1992b):

- 1- the outer hydrogen layer of GD 154 could be thinner: modes of higher k index are trapped,
- 2- the convection in the outermost layers of GD 154 could be more efficient (equivalent to a lower effective temperature),
- 3- GD 154 could be a low mass DA.

From Bergeron et al. (1995), it is known that the third hypothesis is obviously not the right one (they derive a mass of $0.70 M_{\odot}$ for GD 154 against $0.55 M_{\odot}$ for G 38-29 and $0.63 M_{\odot}$ for R 808); the fact that GD 154 is the most massive of the three stars reinforces the first two assumptions.

Since the best fit for the optical and UV spectra was obtained for a unique version of the mixing length theory (MLT) ($ML2/\alpha=0.6$), there is no special reason to believe that GD 154 should behave differently than other ZZ Ceti stars. Finally, one is left with the only explanation that GD 154 has the longest period because of its thin hydrogen envelope.

For the above mentioned arguments, GD 154 was considered to be an interesting target for a WET campaign. Such a campaign was organized in 1991 and the observations are described in § 2. The power spectrum and the inferred rotational splitting are discussed in § 3 and § 4, respectively. An interpretation is given in § 5. The main conclusions of the paper are summarized in § 6.

2. Observations

GD 154 ($\alpha_{2000} = 13^{\text{h}}09^{\text{m}}58^{\text{s}}$, $\delta_{2000} = +35^{\circ}09'5''$) was one of the two first priority targets of the May 1991 WET observing run. 162.5 h of data have been collected over 12 days from six observatories distributed in longitude (see Table 1 for the Journal of the observations). The resulting resolution in the frequency domain is $1 \mu\text{Hz}$.

The method of data acquisition and reduction is described in Nather et al. (1990). In the two sites, where 3-channel photometers were used, the third channel was continuously observing the sky

background. For these data, the sky is subtracted on a point by point basis.

In all other data, obtained with 2-channel photometers the observations of the target and the comparison star were interrupted to sample the sky brightness at irregular intervals as sky conditions warranted.

The sky background contribution is then interpolated and subtracted. The effect of extinction and other low frequency transparency variations were accounted for by fitting a third order polynomial to each sky-subtracted data set and then dividing by this fit.

The light curve is then derived in terms of fractional amplitude: this method allows to use the star as its own magnitude calibration for each telescope. The data obtained on the nearby comparison star in channel 2 are used to measure sky transparency. All light curves are sampled with a 10 s integration time.

All data contaminated by clouds were discarded. Since no telescopes in Asia were used and this WET campaign had two twin primary targets, the duty cycle for the whole campaign is only 48.8 %.

The data have been placed on a common BJD time scale. Barycentric correction was applied on each data point in order to correct the time delay introduced by the heliocentric motion of the Earth during the light curve acquisition. The final product of the basic reduction procedures is shown in Fig. 1.

3. The power spectrum

Fig. 2a gives the discret Fourier transform of the entire WET campaign. In Fig. 2b the corresponding spectral window is shown, which is the power spectrum of a sinus function sampled in the same way as the data. To make the comparison with the observed power spectrum easier, the amplitude and the frequency of the sinus function was choosen equal to that of the main peak in Fig. 2a.

The power spectrum does not exhibit any significant signal for frequencies higher than 5 mHz. The noise level of the observed power spectrum begins to rise, roughly exponentially, below 0.5 mHz, thus diluting any signal that might be present.

In order to scrutinize deeper in the WET power spectrum , and to distinguish real peaks from the false ones introduced by the side-lobes of the spectral window, it has been deconvolved using two dif-

Table 1. Journal of observations of the WET campaign

Observatory and telescope	Date (May 91)	Started at	Length
		(UT) h m s	(s)
McDonald 2.08 m	13	06:09:30	12100
McDonald 90 cm	14	03:41:00	10980
McDonald 2.08 m	15	03:19:00	9880
Mauna Kea 60 cm	15	06:10:20	2290
McDonald 2.08 m	15	07:30:10	7640
Mauna Kea 60 cm	15	08:11:50	17720
La Palma 2.54 m	16	00:27:30	13015
McDonald 90 cm	16	02:55:00	23305
Mauna Kea 60 cm	16	07:31:50	23400
Wise 1 m	16	18:35:11	1785
Wise 1 m	16	19:48:01	3635
H. Provence 1.93 m	16	21:48:37	16070
McDonald 90 cm	17	03:00:00	10775
Mauna Kea 60 cm	17	06:10:20	26415
Mc Donald 90 cm	17	06:15:00	2735
Mc Donald 90 cm	17	07:41:15	7260
Wise 1 cm	17	18:44:01	2005
Wise 1 cm	17	19:30:31	5830
H. Provence 1.93 m	17	20:59:30	18900
Wise 1 m	17	21:50:21	2220
McDonald 90 cm	18	02:57:00	15745
Mauna Kea 60 cm	18	05:59:20	29005
H. Provence 1.93 m	18	20:51:50	19020
Itajuba 1.60 m	19	01:23:10	14630
McDonald 90 cm	19	02:59:00	23300
Mauna Kea 60 cm	19	06:53:20	26070
H. Provence 1.93 m	19	21:05:30	16440
McDonald 90 cm	20	03:04:20	22510
Mauna Kea 60 cm	20	05:50:30	24150
Mauna Kea 3.58 m	20	06:33:23	9990
H. Provence 1.93 m	20	21:09:00	18005

Table 1 (Continued)

Observatory and telescope	Date (May 91)	Started at (UT) h m s	Length (s)
Mauna Kea 60 cm	21	09:51:00	13370
Wise 1 m	21	18:34:10	2025
H. Provence 1.93 m	21	21:01:00	18968
Mauna Kea 3.58 m	22	05:49:40	21600
H. Provence 1.93 m	22	21:26:40	17640
McDonald 2.08 m	23	05:52:00	7720
Mauna Kea 3.58 m	23	06:04:37	14400
McDonald 2.08 m	24	03:41:10	10275
Mauna Kea 3.58 m	24	05:51:43	20920
McDonald 90 cm	25	03:15:00	21215

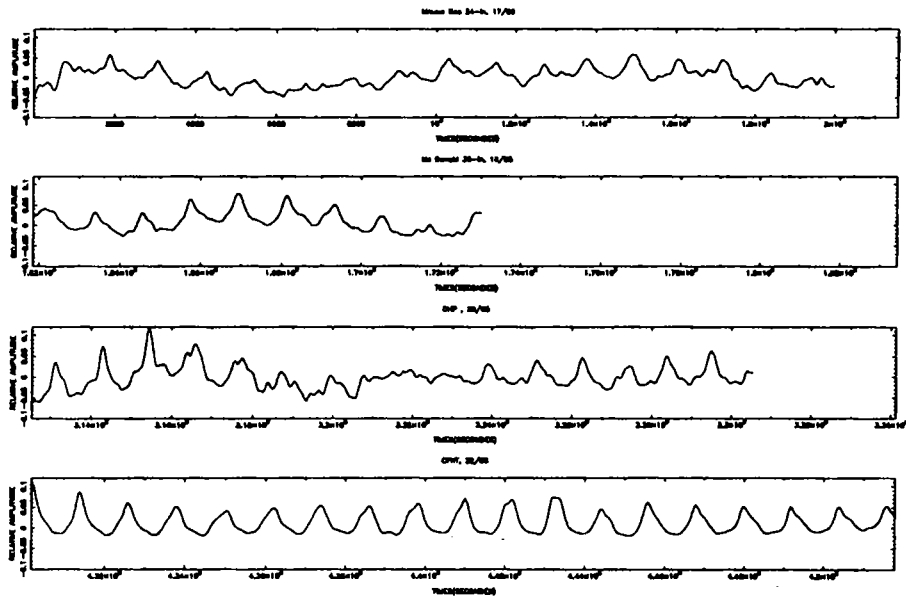


Fig. 1. The final product of the basic reduction procedures.

ferent methods, one of them running in the time domain (ISWF, Ponman 1981), and the second one running in the dual domain (based on the CLEAN method, Högbom, 1974). In each case, all the peaks be-

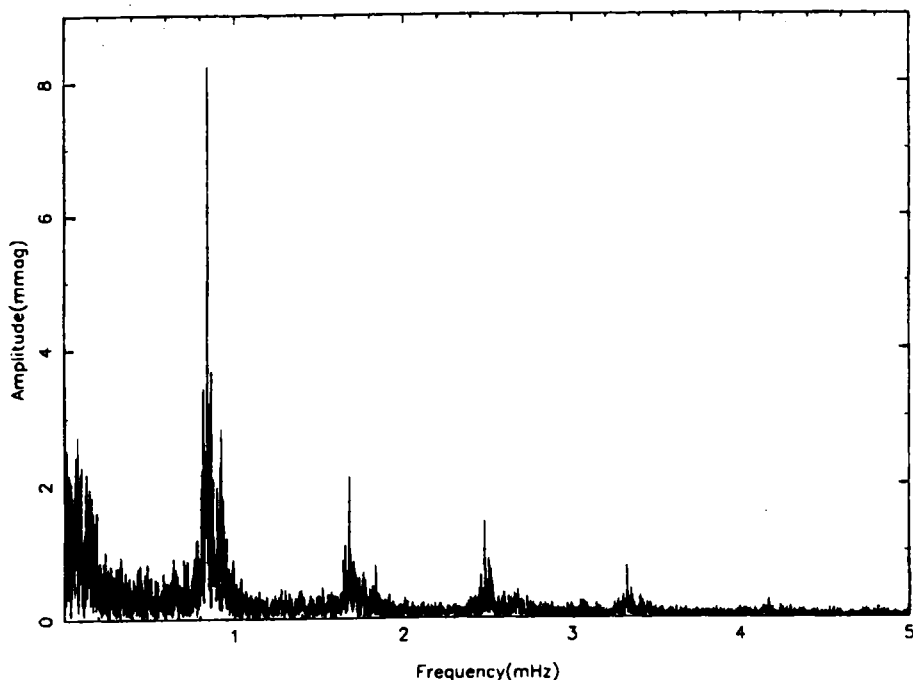


Fig. 2a. Discret Fourier transform of the entire WET campaign.

longing to a given "forest" of peaks are deconvolved simultaneously in order to avoid propagating errors in the computation of the amplitudes and phases of the injected sinus waves. Both methods gave compatible results. Table 2 gives the list of frequencies, periods and amplitudes of all peaks extracted from the WET power spectrum by the described procedures.

The WET spectrum is dominated by the three independent modes: $f_1 = 842.8 \mu\text{Hz}$, $f_2 = 918.6 \mu\text{Hz}$ and $f_3 = 2484.1 \mu\text{Hz}$. All other peaks, except two can be interpreted as harmonics and linear combinations of these three main peaks. The frequencies f_1 and f_2 appear to be triplets which will be discussed below (§ 4). The frequency f_3 is close to the second harmonic of f_1 ($3f_1 = f_3 + 44.3 \mu\text{Hz}$) so that linear combinations of f_1 and f_3 can mimic high order harmonics of f_1 in lower resolution data.

A comparison of the WET spectrum with the previous observations performed 14 years earlier by Robinson et al. (1978), reveals drastic changes. The power spectrum was then dominated by a single mode and its integer, and half-integer harmonics. It could also be

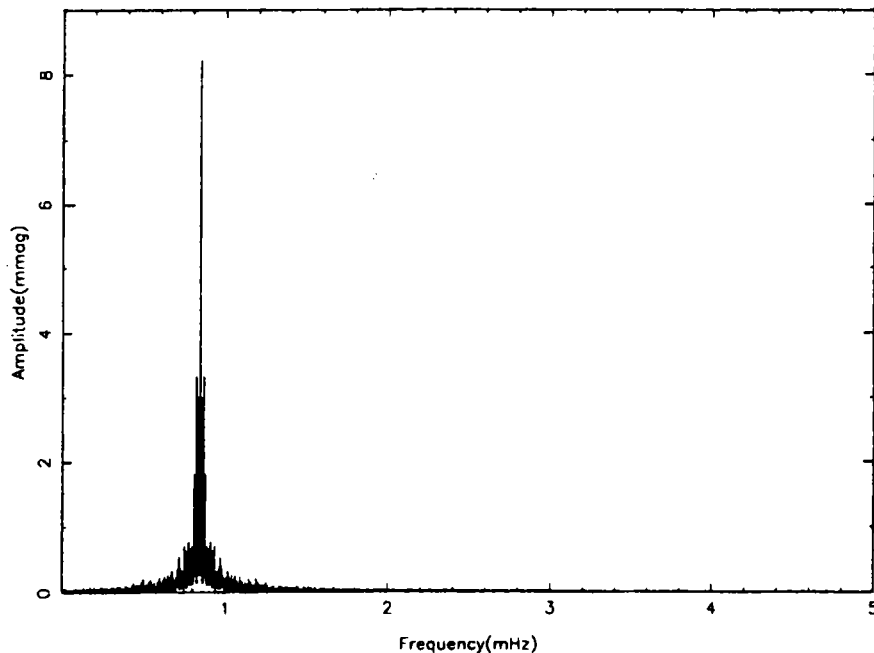


Fig. 2b. Spectral window – the power spectrum of a sinus function sampled in the same way as the data.

interpreted as two modes (f_1 and $1.52f_1$) and their harmonics and linear combinations. In the WET data, two new modes appear, one close to f_1 (f_2) and the other one close to $3f_1$ (f_3). The striking result of the WET campaign is that there is no evidence of peaks around $1.52f_1$, not even in the power spectra of individual nights.

4. The rotational splitting

As one can see from Table 2, the WET observations reveal that the large amplitude region around f_1 ($842.8 \mu\text{Hz}$) is seen to split into a triplet whose components are hereafter referred to as f_1^- , f_1 and f_1^+ . This triplet is almost symmetric in amplitude and the frequency separations are $f_1 - f_1^- = 2.8 \mu\text{Hz}$ and $f_1^+ - f_1 = 2.2 \mu\text{Hz}$. It is interpreted as rotational splitting of a g-mode $\ell = 1$. For such a large period, one can reasonably assume that the asymptotic regime (large k) is reached. After setting $\delta f_1 = 2.5 \mu\text{Hz}$ (average of the above

Table 2. Frequencies, periods and amplitudes of WET power spectrum peaks

Frequency (μHz)	Period (s)	Amplitude (%)	Interpretation
840.0	1190.5	0.63	f_1^-
842.8	1186.5	1.67	f_1
845.0	1183.5	0.46	f_1^+
915.7	1092.1	0.30	f_2^-
918.6	1088.6	0.50	f_2
922.5	1084.0	0.56	f_2^+
1683.2	594.1	0.39	$(2.f_1^-)$
1686.2	593.1	0.21	$2f_1$
1759.9	568.2	0.11	$f_1 + f_2$
1765.2	566.5	0.13	$f_1 + f_2^+$
1823.4	548.4	0.11	—
1837.7	544.2	0.18	$2f_2$
2484.1	402.56	0.27	f_3
2518.6	397.05	0.08	$3.f_1^-$
2526.2	395.86	0.09	$(3f_1)$
2597.5	384.98	0.08	$2f_1^- + f_2$
2680.2	373.10	0.08	$f_1 + 2f_2$
3323.3	300.90	0.07	$f_3 + f_1 m$
3327.0	300.57	0.16	$f_3 + f_1$
3406.4	293.57	0.06	—
3448.4	289.99	0.05	$3f_1 + f_2$
4169.8	239.82	0.06	$f_3 + 2f_1$

frequency separations), one can obtain a straightforward derivation of the rotation period of the star:

$$P_{\text{rot}} = \frac{1}{2.\delta f_1} = 2.3 \text{ d} .$$

The mode f_1^- can be interpreted as the $m = -1$ component of the triplet, f_1 as the $m = 0$ component and f_1^+ as the $m = +1$ component. The frequency asymmetry is marginally significant; we will not try to overinterpret it.

The WET data reveal that the peak f_2 is composed of two components: f_2 (918.6 μHz) and f_2^+ (922.5 μHz) separated by 3.9 μHz . After subtraction of these two components, the power spectrum exhibits a third component at 915.7 μHz . However, this deconvolution gives a low level of confidence to measurements of the frequency and amplitude of the peak f_2^- , as the window function has high sidelobes and because one has to deconvolve two peaks of higher amplitude (f_2 and f_2^+) before being able to detect f_2^- .

5. Interpretation

Since only three independent eigenmodes are distinguished in GD 154, it is not possible to estimate the mass by computation of its average period spacing. The reduced number of observed eigenmodes does not give enough constraints to determine the basic physical parameters of this object by comparing its eigenperiod distribution with pulsating white dwarf models. In order to give an interpretation of the observed power spectrum, one needs to impose other constraint by assuming that the observed modes are selected among the rich period spectrum of the star by a mode trapping in the outer hydrogen layer (Winget et al. 1981, Dolez & Vauclair 1981, Winget & Fontaine 1982).

In the framework of this hypothesis and assuming that the mode f_1 (period P_1) is $\ell = 1$, one can try to determine the value of the ℓ index of the mode f_2 (period P_2). First, let us assume that f_2 is a mode $\ell = 1$. Then, the difference of the reduced periods between P_1 and P_2 is:

$$\Delta P = \sqrt{2}(P_1 - P_2) = 138.5 \text{ s} .$$

According to Brassard et al. (1992a), the difference of reduced periods between two successive trapping valleys, Π_H , ranges from ~ 475 s to ~ 660 s, depending on the parameter of the model (stellar mass M_* , hydrogen layer thickness M_H , effective temperature (T_{eff}) and convection efficiency (described by the λ_i coefficients)). So, P_1 and P_2 are too close to allow these two modes to belong to two successive trapping valleys. Comparison of ΔP with that, given by the Brassard models, shows that P_2 is too large to be the mode $\ell = 1$

adjacent to P_1 , partially trapped in the valley of P_1 . As f_2 cannot be a trapped $\ell = 1$ mode, it is assumed that P_2 is a mode $\ell = 2$. Assuming that f_2 and f_2^+ are two modes belonging to the same multiplet (same ℓ , consecutive m), one can notice that the ratio of the frequency separations in the multiplets f_1 and f_2 is close to the theoretical ratio expected for a multiplet $\ell = 1$ and a multiplet $\ell = 2$ in the asymptotic regime ($\delta f_{\ell=1}/\delta f_{\ell=2} = 0.6$):

$$\frac{\delta f_1}{\delta f_2} = \frac{2.5}{3.9} = 0.64 .$$

This reinforces the hypothesis that f_2 is a mode $\ell = 2$. The mode f_2 can be the $m = 0$ component of this asymmetric multiplet, the mode f_2^+ corresponds to $m = +1$ and f_2^- to $m = -1$. Other components of the multiplets ($m = \pm 2$) are not detected.

The frequency asymmetry of multiplets is frequently observed in DAVs power spectra. In the case of noisy data and high side-lobe spectral window, one must be careful not to overinterpret such an asymmetry, as it can be due to deconvolution errors. It should be emphasized that finding a family of frequencies, amplitudes and phases that enable us to compute a synthetic power spectrum very "similar" to the observed one does not *prove* that the obtained solution is the best one. This problem is crucial in the case of noisy data where one can find many solutions enabling to produce a synthetic power spectrum, similar to the observed one.

The amplitude asymmetry of multiplets is also often observed in DAVs power spectra. Here, the triplets are too strongly asymmetric to allow an estimate of the angle between the axis of pulsations and the line of sight (as proposed by Pesnell 1985).

Having identified the modes f_1 and f_2 as $\ell = 1$ and $\ell = 2$ modes, one can try to identify the ℓ index of the mode f_3 (period P_3). The periods of trapped modes of the same degree ℓ must verify:

$$\frac{P_{i_1\ell}}{P_{i_2\ell}} = \frac{\lambda_{i_1}}{\lambda_{i_2}}$$

where λ_i were derived independently by Kawaler and Weiss (1991) and Brassard et al. (1992a). Here, the period ratios are:

$$\frac{P_2}{P_3} = 2.70 \quad \text{and} \quad \frac{P_1}{P_3} = 2.95.$$

The only ratio of λ_i , which can match the observed ratios, is λ_3/λ_1 . All the other values correspond to trapping valleys so that $i_2 - i_1 \geq 6$ which would imply so short a period cycle between trapped modes (Π_H) that they can immediately be discarded. Taking the efficiency of the convection in the model and assuming that the effective temperature of GD 154 is 11 200 K, one can derive from Brassard et al. (1992a) :

$$\lambda_3/\lambda_1 = 2.73 \text{ for ML1 and } \lambda_3/\lambda_1 = 2.97 \text{ for ML3.}$$

One can conclude that either: (1) the modes f_2 (period P_2) and f_3 (period P_3) have the same ℓ index ($\ell = 2$), their trapping indexes being equal to 3 and 1, respectively, and the convection efficiency is ML1, or (2) the modes f_1 (period P_1) and f_3 (period P_3) have the same ℓ index ($\ell = 1$), their trapping indexes being equal to 3 and 1, respectively, and the convection is very efficient (ML3).

A glance to Fig. 15 of Brassard et al. (1992a) allows us to discard the first case (impossibility of finding a model reproducing the correct period ratio and the existence of a mode $\ell = 1$ with a period ~ 1200 s, even if one explores this diagram for stellar masses larger than $0.6 M_\odot$). According to Clemens (1993), considerations based on the comparison of spectra of 24 known stars of the ZZ Ceti type also give clues that the mode P_3 is an independent $\ell = 1$ mode.

The conclusion follows, that the assumption (2) must be the correct one. The mode f_3 (period P_3) should be a $\ell = 1$ mode. The modes f_1 and f_3 are both $\ell = 1$ g-modes with trapping index $i = 3$ and $i = 1$ respectively while f_2 is a $\ell = 2$ mode. Period ratio arguments do not affect a value of the i trapping index for the mode f_2 . If this interpretation is correct, it does not agree with the earlier suggestion by O'Donoghue (1986) that the short time variation observed by Robinson et al. (1978) could appear due to beating of higher ℓ degree multiplets.

One could ask: why is the trapped mode $\ell = 1$, $i = 2$ not observed? If one computes, according to Brassard et al. (1992a), the ratio λ_3/λ_2 for the model with $T_{\text{eff}} = 11\,200$ K and a convective efficiency ML3, one finds:

$$\frac{\lambda_3}{\lambda_2} = 1.49 .$$

It is tempting to suggest that the $1.52f_1$ mode observed by Robinson et al. (1978) which is remarkably absent in the WET data is precisely the mode $\ell = 1$, $i = 2$ with frequency $1.49f_1$. In this case, the "half-integer" subharmonics observed by Robinson et al. (1978) are the

linear combinations of the frequencies of two $l = 1$ trapped modes: the main mode (f_1), corresponding to the third trapping valley ($i = 3$), and the mode $1.52f_1$, corresponding to the second trapping valley ($i = 2$).

Table 3. Identification of the independent eigenmodes in GD 154

Mode	l	m	i
f_1^-	1	-1	3
f_1	1	0	3
f_1^+	1	+1	3
f_2^-	2	-1	-
f_2	2	0	-
f_2^+	2	+1	-
$1.52f_1$	1	-	2
f_3	1	-	1

Since the ℓ and i indices of the main mode are identified, one can derive from relation (28) of Brassard et al. (1992a) that:

$$\left(\frac{M_\star}{M_\odot}\right)^{1.079} \left(\frac{M_H}{M_\star}\right)^{0.102} \left(\frac{T_{\text{eff}}}{11\,500\text{ K}}\right)^{0.262} = \frac{1}{14.34}.$$

Using the determination of $T_{\text{eff}} = 11\,180\text{ K}$ and $M_\star = 0.70\,M_\odot$ derived by Bergeron et al. (1995), one obtains:

$$(M_H/M_\star) = 2 \times 10^{-10}.$$

This value of the mass of the hydrogen outer layer makes GD 154 a ZZ Ceti type star having the thinnest hydrogen envelope so far. With such a thin hydrogen layer, the mode trapping in GD 154 should be very efficient. This sustains the basic assumption that the three modes observed in GD 154 are trapped modes of high k order. It also confirms what was suspected in the introductory part of this paper: modes of very large periods are excited in GD 154 because this massive DAV star has a thin hydrogen layer and, possibly, a high convection efficiency. However, the mass of this hydrogen layer is still too large for supporting the assumption that the red edge could be due to convective mixing of the outer hydrogen with the helium underneath.

6. Conclusions

The Whole Earth Telescope has proven its ability to perform a detailed asteroseismological investigation of a variable DA white dwarf. During the WET observations, the behavior of GD 154 was dominated by three independent eigenmodes. Under the assumption that all these modes are trapped in the outer hydrogen layer, an identification of their asteroseismological indices ℓ and i was possible, as well as the indices of the eigenmode observed 14 years ago by Robinson et al. (1978). These identifications are summarized in Table 3. With the help of two more constraints derived from spectroscopic measurements by Bergeron et al. (1995) (T_{eff} and M_*), an estimate of the hydrogen layer mass $M_{\text{H}} = 2 \times 10^{-10} M_*$ is proposed.

In future, the behavior of this object (using monosite campaigns) should be followed carefully in order to detect new drastic changes in its pulsation modes. New tools have also to be developed to understand its non-linear behavior: accurate time-frequency analysis enabling to describe quantitatively the amplitude variations of the individual modes and theoretical tools to describe the nonlinear terms observed in the power spectrum of this object.

References

- Bergeron P., Wesemael F., Lamontagne R., Fontaine G., Saffer R.A., Alard N.F. 1995, ApJ, in press
Brassard P., Fontaine G., Wesemael F., Hansen C.J. 1992a, ApJS, 80, 369
Brassard P., Fontaine G., Wesemael F., Tassoul M. 1992b, ApJS, 81, 747
Clemens J.C. 1993, private communication
Daou D., Wesemael F., Bergeron P., Fontaine G., Holberg J.B. 1990, ApJ, 364, 242
Dolez N., Vauclair G. 1981, A&A, 102, 375
Goupil M.-J., Auvergne M., Baglin A. 1988, A&A, 196, L13
Högbom, J.A. 1974, A&AS, 15, 417
Kawaler S.D., Weiss P. 1991, in Progress of Seismology of the Sun and Stars, Proc. of the 9th International Seminar, Springer-Verlag, Berlin
Kepler S.O., Nelan E.P. 1993, AJ, 105, 608
Nather R.E., Winget D.E., Clemens J.C., Hansen C.J., Hine B.P. 1990, ApJ, 361, 309
O'Donoghue D. 1986, MNRAS, 220, 19P
Pesnell W.D. 1985, ApJ, 292, 238
Ponman T. 1981, MNRAS, 196, 583

- Robinson E.L., Stover R.J., Nather R.E., McGraw J.T. 1978, *ApJ*, 220, 614
- Vauclair G., Goupil M.-J., Baglin A., Auvergne M., Chevreton M. 1989, *A&A*, 215, L17
- Winget D.E., van Horn H.M., Hansen C.J. 1981, *ApJ*, 245, L33
- Winget D.E., Nather R.E., Hill A.J. 1987, *ApJ*, 316, 305
- Winget D.E., Fontaine G. 1982, in *Pulsations in Classical and Cataclysmic Variable Stars*, eds. J.P. Cox & C.J. Hansen, University of Colorado, Boulder, p. 46
- Winget D.E. 1988 , in *Advances in Helio- and Asteroseismology* (IAU Symp. No. 123), eds. J. Christensen-Dalsgaard & S. Frandsen, Reidel, p. 305